

303633

An Investigation of the Processes Controlling
Ozone in the Upper Stratosphere

Kenneth O. Patten, Jr., Peter S. Connell, Douglas E. Kinnison, Donald J. Wuebbles
Lawrence Livermore National Laboratory
Livermore, CA 94550, USA

Joe Waters, Lucien Froidevaux
Jet Propulsion Laboratory
Pasadena, CA 91109, USA

and

Tom G. Slanger
SRI International, Inc.
Menlo Park, CA 94025, USA

ABSTRACT

Photolysis of vibrationally excited oxygen produced by ultraviolet photolysis of ozone in the upper stratosphere is incorporated into the Lawrence Livermore National Laboratory 2-D zonally averaged chemical-radiative-transport model of the troposphere and stratosphere. The importance of this potential contributor of odd oxygen to the concentration of ozone is evaluated based upon recent information on vibrational distributions of excited oxygen and upon preliminary studies of energy transfer from the excited oxygen. When the energy transfer rate constants of previous work are assumed, increases in model ozone concentrations of up to 40 percent in the upper stratosphere are found, and the ozone concentrations of the model agree with measurements, including data from the Upper Atmosphere Research Satellite. However, the increase is about 0.4 percent when the larger energy transfer rate constants suggested by more recent experimental work are applied in the model. This indicates the importance of obtaining detailed information on vibrationally excited oxygen properties to evaluation of this process for stratospheric modeling.

INTRODUCTION

Simulations of stratospheric chemistry do not produce as large an ozone concentration as is experimentally found in the upper stratosphere. This difference has been known for at least 15 years (Butler, 1978; WMO, 1985). One of the possible explanations of this lower ozone concentration is that a source of odd oxygen is missing from the existing models. Slanger *et al.* (1988) have proposed a possible additional source of odd oxygen based on experiment. Photodissociation of ozone in the ultraviolet (200 to 310 nm) produces oxygen molecules in the ground electronic state. This oxygen carries a large vibrational excitation (Slanger *et al.*, 1988; Kinugawa *et al.*, 1990). The vibrationally excited oxygen ($O_2^*(v)$) then absorbs a second photon by its Schumann-Runge transition and dissociates to two O atoms. This second dissociation can occur with light considerably to the red of that which photolyzes thermal oxygen. In order to incorporate this mechanism into atmospheric models, the distribution of O_2^* with respect to vibrational quantum number v and the rate constants for removal of vibrational quanta from O_2^* by collisional quenching must be known.

Utilizing O_2^* distributions from Kinugawa *et al.* (1990) and quenching rate constants for O_2^* based on Rapp (1965), Toumi *et al.* (1991) found an enhancement of ozone concentration ranging from 13 to 60 percent for altitudes of 36 to 58 km in their atmospheric model. The 248 nm O_3 photolysis data of Slanger (private communication) indicate a different $O_2^*(v)$ distribution, and preliminary collisional quenching data in the same study indicate a considerably higher rate constant than was used previously. Photolysis of O_2^* has been incorporated into the LLNL global two-dimensional chemical-radiative-transport model, and this study compares the ozone concentrations calculated using both the earlier collisional quenching and the experimental quenching with observed ozone concentrations, including recent measurements from the Upper Atmosphere Research Satellite Microwave Limb Sounder (UARS MLS).

EXCITED OXYGEN CHEMISTRY

The LLNL 2-D model has been discussed previously (Johnston *et al.*, 1989). In addition to the standard model, the rate of photolysis of O_3 into the ground state oxygen channel ($O_2(^3\Sigma_g^-)$) is used to calculate O_2^* processes. As is detailed below, the O_2^* calculation internally performs three steps for each altitude-latitude combination. The nascent distribution of $O_2^*(v)$ is first found from O_3 photolysis rates. Rate constants for O_2^* photolysis are calculated from absorption cross sections. Finally, with the photolysis and energy transfer rate constants, the steady state concentration of $O_2^*(v)$ is determined.

When O_3 is photolyzed, excess energy is distributed among translation (between the centers of mass of O_2 and O atom) and rotation and vibration of the O_2 fragment. Data obtained by Slanger indicate that a bimodal distribution of vibrationally excited O_2 arises when O_3 is photolyzed at 248 nm. The time-of-flight study of Kinugawa *et al.* (1990) shows two peaks of O atom with respect to translational energy when O_3 is photolyzed at 226 nm. The peak at higher O_2 vibrational quantum number is assigned as partially but not completely due to thermal decomposition of O_3 . We use a double Gaussian fit in the relative translational energy of photolysis fragments to approximate both the Slanger data and the Kinugawa *et al.* data. Since the vibrational energy in $O_2(^3\Sigma_g^-)$ is equal to the photolysis energy minus E_r except for the rotational energy in O_2 , the vibrational distribution can be calculated.

The O_2^{\dagger} cross sections are calculated from wavefunctions for O_2 and the Schumann-Runge transition dipole moment function using equations based on those in Levine (1975) and Saxon and Slanger (1991). The wavefunctions for both the ground and excited electronic states are calculated from potential surfaces using the method of Kulander (1988). The Rydberg-Klein-Rees potential surfaces of ground O_2 ($^3\Sigma_g^-$) and excited O_2 ($^3\Sigma_u^-$) are from Krupenie (1972) extrapolated to $r = 1.0 \text{ \AA}$ and to $r = 11.0 \text{ \AA}$. The transition dipole moment function $D(r)$ is from Allison *et al.* (1986). The transition strengths produced agree to within 50% with the experimental transition strengths of Lewis *et al.* (1986) and calculated transition strengths of Allison *et al.* (1971). Cross sections agree reasonably with the $v = 12$ cross sections found by Saxon and Slanger (1991).

The removal of vibrational excitation from O_2^{\dagger} involves multiple processes which ultimately must be distinguished from one another. The O_2^{\dagger} may lose vibrational excitation by either transfer to translational and rotational energy or transfer to vibrational energy. Either transfer mechanism preferentially removes one quantum of vibrational energy; however, according to Slanger's preliminary observations on O_2^{\dagger} collisions with nitrogen for $v = 18$ to 20, processes which remove two quanta of vibrational energy from O_2^{\dagger} are also significant. Further work at $v = 22$ finds that nitrogen and oxygen have approximately the same rate constants for O_2^{\dagger} quenching, so that v - v transfer must dominate there. A model proposed by Rapp and Englander-Golden (1964) and by Rapp (1965), as further expanded to multiple-quantum removal by Yardley (1980), provides the v - v energy transfer rate constants used in the O_2^{\dagger} model. The v - t contribution chosen for compatibility with the Slanger *et al.* observations at $v = 22$ is $3.0 \times 10^{-15} \text{ molec cm}^{-3} \text{ s}^{-1}$ for all temperatures and for both $M = O_2$ and $M = N_2$; this is referred to as the "full k_c case" in the results. The sensitivity of the O_2^{\dagger} processes to the choice of energy transfer rate constants must be determined due to the preliminary nature of the Slanger group results. A second

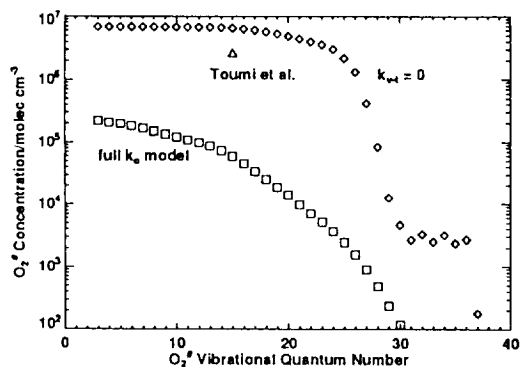


Figure 1. Steady state concentrations of vibrationally excited oxygen versus vibrational quantum number for 30° N, 44 km on the Autumn Equinox for both zero vibration-to-translation contribution (\diamond) and the full vibrational energy transfer model (\square) are compared with the result of Toumi *et al.* (1991) for $v = 15$ (\triangle).

series of 2-D model runs is thus conducted with $k_{v,t}$ set to zero and $M = O_2$ alone; this lower limit to the uncertainty range of O_2^{\dagger} energy transfer rate constants is referred to as the " $k_{v,t} = 0$ " case below. The rate constants of this case are similar to those used by Toumi *et al.* (1991).

O_2^{\dagger} may be either deactivated by collisional energy transfer or photolyzed in the Schumann-Runge transition region. The lifetime of O_2^{\dagger} is less than one hour, so that the instantaneous equilibrium or steady-state approximation may be applied to each of the species $O_2^{\dagger}(v)$. Those equations are solved using the fact that O_2^{\dagger} may not be produced with v greater than its dissociation limit of 38.

MODEL-DERIVED O_2^{\dagger} AND O_3

Figure 1 illustrates steady state O_2^{\dagger} concentrations (Equation 4) at noon on the Autumn Equinox (September 22) in the LLNL 2-D model with respect to vibrational quantum number. In the $k_{v,t} = 0$ model (diamonds), the concentration of O_2^{\dagger} falls off rapidly for $v > 25$ from values of at least $5 \times 10^6 \text{ molec cm}^{-3}$ which remain nearly constant with v . Use of the full k_c model (squares) reduces the maximum O_2^{\dagger} concentration to $2 \times 10^5 \text{ molec cm}^{-3}$ for $v = 3$, and the concentration decreases more steeply throughout the range of v , reaching $2 \times 10^3 \text{ molec cm}^{-3}$ at $v = 25$. The additional quenching of the full k_c model severely reduces the calculated O_2^{\dagger} concentrations and will be shown to reduce the O_2^{\dagger} effect upon odd oxygen considerably compared with that of Toumi *et al.* (1991). Toumi *et al.* (1991) provides $[O_2^{\dagger}]$ only for $v = 15$ (triangle), which is slightly less than is the $[O_2^{\dagger}(15)]$ for our $k_{v,t} = 0$ case in Figure 1.

The rate of O atom production from O_2^{\dagger} also depends on the rate of O_3 photolysis, the solar flux, and the absorption cross section of O_2^{\dagger} . For both k_c models, the rate of O_2^{\dagger} photolysis in $\text{molec cm}^{-3} \text{ s}^{-1}$ (one half of the O atom production rate) at 30°N, Autumn Equinox noon is plotted against v in Figure 2. The O_2^{\dagger} photolysis rate peaks at $2 \times 10^5 \text{ molec cm}^{-3} \text{ s}^{-1}$ for $v = 20$ in the $k_{v,t} = 0$ model, with considerable contributions for v down to 12 and up to 27. However, in the full

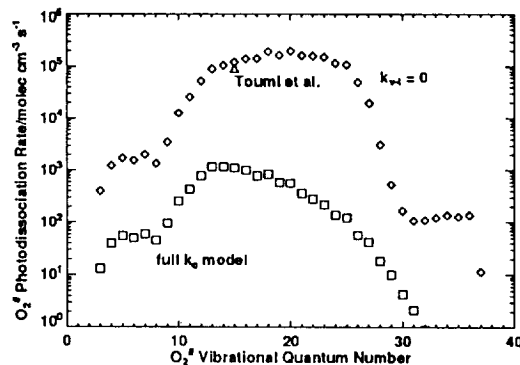


Figure 2. Rate of photolysis for vibrationally excited oxygen versus vibrational quantum number for 30° N, 44 km on the Autumn Equinox. Zero vibration-to-translation case: \diamond ; full vibrational energy transfer model: \square ; Toumi *et al.* (1991) for $v = 15$: \triangle .

k_0 model, the maximum contribution becomes 1×10^3 molec $\text{cm}^{-3} \text{s}^{-1}$ at $\nu = 12$, and the photolysis rate falls off more quickly with ν to either direction. The strongest contribution to O atom production from O_2^+ comes from ν in the range of 10 to 25, and the higher ν are most severely affected by use of the full k_0 quenching both in terms of concentration and in terms of photolysis rate.

Figure 3 illustrates the ratio of the O_2^+ dissociation rate to the thermal O_2 dissociation rate at the Autumn Equinox. The altitude shown is the log-pressure scaled altitude used in the 2-D model. Altitudes less than 30 km are omitted for this figure and Figure 4 since neither process is significant. In the $k_{v,1} = 0$ case (Figure 3A), the O_2^+ process contributes 10 percent as much odd oxygen as does thermal O_2 photodissociation around 35 km for all latitudes except the Antarctic region. The odd oxygen addition from O_2^+ increases with increasing altitude up to 55 km. Peak values of the ratio are greater than 50 percent at latitudes of 45 °S and 60 °N and 55 km altitude. Toumi *et al.* (1991) Table 2 shows an odd oxygen production ratio at 30 °N on the Autumn Equinox which increases monotonically from 13 percent at 36 km to 60 percent at 58 km, but with a leveling off of the rate of increase with altitude at the higher altitudes. Some quantitative differences in the production ratio exist between our model and that of Toumi *et al.*, but the qualitative features are mostly the same at 30 °N.

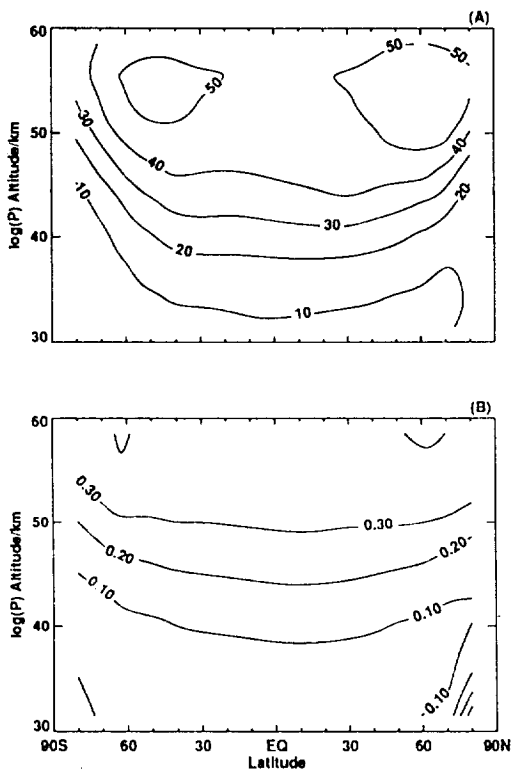


Figure 3. Ratio (percent) of rate of photolysis (molec $\text{cm}^{-3} \text{s}^{-1}$) of O_2^+ to that of thermal O_2 for (A) $k_{v,1} = 0$ case; (B) full k_0 case.

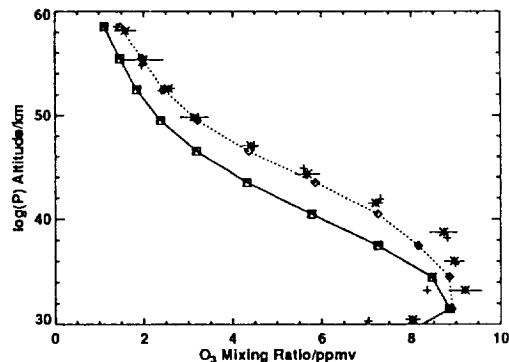


Figure 4. Comparison of LLNL 2-D model results with measurements of ozone concentration on the Autumn Equinox at 30° N. * - UARS MLS (lines represent 1 σ uncertainty); + - MAP recommended values (10 percent typical uncertainty); Δ - LLNL 2-D ambient atmosphere (no O_2^+); \diamond - LLNL 2-D model, $k_{v,1} = 0.0 \text{ cm}^3 \text{ molec}^{-1} \text{ s}^{-1}$, O_2 v-v transfer only; \square - LLNL 2-D model, $k_{v,1} = 3.0 \times 10^{-15} \text{ cm}^3 \text{ molec}^{-1} \text{ s}^{-1}$, N_2 and O_2 colliders.

The full k_0 case (Figure 3B) reduces the odd oxygen percentage ratio from O_2^+ compared with thermal O_2 by two orders of magnitude for all latitudes and altitudes. Increased collisional quenching forces the maximum O_2^+ production upward (lower pressure), so that the maximum of 0.4 percent is located at 58 km, 60 °S or 60 °N; the upper limit of the model is at 58 km, so that this is not necessarily the overall maximum, but contributions for higher altitudes should not be markedly larger due to decreasing concentrations of O_3 . The contribution of O_2^+ below 58 km is sharply reduced at all latitudes toward a minimum of less than 0.1 percent about 40 km. O_3 concentrations for an ambient atmosphere in our 2-D model also typically change by 0.1 percent from year to year.

Addition of approximately half again as much O atom from O_2^+ as is produced by thermal O_2 photolysis in the $k_{v,1} = 0$ case to the upper stratosphere should produce a large increase in O_3 concentration. Figure 4 compares model O_3 concentrations on the Autumn Equinox at 30°N as a function of altitude with preliminary results from UARS MLS and the recommended zonal mean values of the Middle Atmosphere Program (Keating *et al.*, 1989). When $k_{v,1} = 0$ is used (diamonds), the O_3 concentration is markedly greater for all altitudes above 32 km than for the ambient atmosphere. The resulting concentrations are within the uncertainty limits of the preliminary measurements of the UARS MLS and are comparable to the MAP recommended values for September at 30 °N (crosses) for log-pressure altitudes down to 44 km. The MLS measurements are an average over 28 °N to 32 °N for September 21, 1991 for the 205 GHz O_3 band. Absolute accuracy of MLS is still under investigation, but the O_3 concentrations observed at these altitudes are not expected to vary significantly. The change between the LLNL 2-D model without O_2^+ processes (triangles) and for the O_2^+ full k_0 case (squares) is insignificant on the scale of Figure 4.

CONCLUSIONS

Odd oxygen production from the photolysis of vibrationally excited oxygen (O_2^f) produced by ultraviolet photolysis of ozone (O_3) in the upper stratosphere has been incorporated in the LLNL 2-D global stratosphere-troposphere model. When quenching of O_2^f only by v-v collisional energy transfer to O_2 is considered, odd oxygen production rates throughout the upper stratosphere (>30 km) increase by up to 50 percent, with a corresponding increase in O_3 concentration, in qualitative agreement with the previous work by Toumi *et al.* (1991). Inclusion of an assumed v-t collisional energy transfer rate constant and of N_2 as a collider gas, indicated by recent preliminary experimental work, reduces the odd oxygen contribution from O_2^f processes to insignificance compared with thermal O_2 photolysis. The sensitivity of O_2^f processes in the stratosphere to detailed energy transfer rate constants is well demonstrated here; unfortunately, these constants are not yet well determined in the laboratory. Thus, this study shows the importance of obtaining detailed experimental information on the input parameters of O_2^f , particularly the rate constant for collisional energy transfer as a function of v, in order to judge the potential importance of O_2^f processes to stratospheric O_3 concentrations.

ACKNOWLEDGMENTS

This work was performed under the auspices of the U. S. Department of Energy by the Lawrence Livermore National Laboratory under contract No. W-7405-Eng-48 and was supported in part by the U. S. Department of Energy (DOE) Office of Health and Environmental Research's Environmental Sciences Division and by the National Aeronautics and Space Administration Upper Atmosphere Research Satellite program. KP also appreciates appointment to the Global Change Distinguished Postdoctoral Fellowships sponsored in part by the U. S. DOE, Office of Health and Environmental Research, and administered by Oak Ridge Associated Universities. We thank R. P. Saxon and D. L. Huestis at SRI International, Inc. for many helpful discussions concerning this study, and K. Kulander and B. P. Lengsfeld of LLNL for use of and guidance in their vibrational wavefunction code.

REFERENCES

- Allison, A. C., A. Dalgarno, and N. W. Pasachoff, 1971: Absorption by Vibrationally Excited Molecular Oxygen in the Schumann-Runge Continuum *Planet. Space Sci.* **19**, 1463-73.
- Allison, A. C., S. L. Guberman, and A. Dalgarno, 1986: A Model of the Schumann-Runge Continuum of O_2 *J. Geophys. Res.* **91**, 10,193-8.
- Butler, D. M., 1978: The Uncertainty in Ozone Calculations by a Stratospheric Photochemistry Model *Geophys. Res. Lett.* **5**, 769-72.
- Johnston, H. S., D. E. Kinnison, and D. J. Wuebbles, 1989: Nitrogen Oxides from High-Altitude Aircraft: An Update of Potential Effects on Ozone *J. Geophys. Res.* **94**, 16,351-63.
- Keating, G. M., M. C. Pitts, and D. F. Young, 1989: Ozone Reference Models for the Middle Atmosphere (New

CIRA) in *Middle Atmosphere Program: Handbook for MAP* **31**, G. M. Keating ed., pp. 1-36.

Kinugawa, T., Sato, T., Arikawa, T., Matsumi, Y., and Kawasaki, M., 1990: Formation of $O(^1P_1)$ Photofragments from the Hartley Band Photodissociation of Ozone at 226 nm *J. Chem. Phys.* **93**, 3289-94.

Krupenic, P. H., 1972: The Spectrum of Molecular Oxygen *J. Phys. Chem. Ref. Data* **1**, 423-534.

Kulander, K. C., 1988: Spectroscopy of SO *Chem. Phys. Lett.* **149**, 392-6.

Levine, I. N., 1975: *Molecular Spectroscopy* (John Wiley and Sons, New York), pp. 306-8.

Lewis, B. R., L. Berzins, and J. H. Carver, 1986: Oscillator Strengths for the Schumann-Runge Bands of $^{16}O_2$ *J. Quant. Spectrosc. Radiat. Transfer* **36**, 209-32.

Rapp, D., and P. Englander-Golden (1964): Resonant and Near-Resonant Vibrational-Vibrational Energy Transfer between Molecules in Collisions *J. Chem. Phys.* **40**, 573-5.

Rapp, D., 1965: Interchange of Vibrational Energy between Molecules in Collisions *J. Chem. Phys.* **43**, 316-7.

Saxon, R. P., and T. G. Slanger, 1991: Relative Contributions of Discrete and Continuum Absorption to the Photodissociation of Vibrationally Excited O_2 ($v = 12-20$) *J. Geophys. Res.* **96**, 17291-5.

Slanger, T. G., L. E. Jusinski, G. Black, and G. E. Gadd, 1988: A New Laboratory Source of Ozone and Its Potential Atmospheric Implications *Science* **241**, 945-50.

Toumi, R., B. J. Kerridge, and J. A. Pyle, 1991: Highly Vibrationally Excited Oxygen as a Potential Source of Ozone in the Upper Stratosphere and Mesosphere *Nature* **351**, 217-9.

WMO, 1985: Comparison of Calculated and Observed Ozone Profiles in *Atmospheric Ozone 1985: Assessment of our Understanding of the Processes Controlling its Present Distribution and Change* (World Meteorological Organization Report Number 16), vol. 2, section 8.2, pp. 420-9.

Yardley, J. T., 1980: *Introduction to Molecular Energy Transfer* (Academic Press, New York).

Note added in proof: After this work was presented, R. Toumi has published "An Evaluation of Autocatalytic Ozone Production from Vibrationally Excited Oxygen in the Middle Atmosphere" in *J. Atmos. Chem.* **15**, 69-77. That report incorporated past experimental quenching results and found ozone enhancements ranging from 0.4 to 11 percent for 40-60 km altitude, depending on various models of the nascent O_2^f distribution from O_3 photolysis.